Porous Carbon Produced in Air: Physicochemical Properties and Stem Cell Engineering

Won Hyuk Suh,* Jeung Ku Kang, Yoo-Hun Suh,* Matthew Tirrell, Kenneth S. Suslick, and Galen D. Stucky*

Aerosol materials synthesis methods[1–9] have been utilized to prepare a distinct platform of spherical composite materials that incorporate sub-100 nanometer features. Nanostructured microspheres (ns-μS) and extended surfaces made up of metal, metal oxides and sulfides such as TiO_2,[10–14] SiO_2,[15–19] Co,[20] Co_3O_4, CuO, NiO,[21] ZrO_2,[22] ZnO,[23,24] Al,[25] Al_2O_3,[26] $BiVO_4$,[27] MoS_2,[28] ZnS,[29,30] as well as polymers[31] and carbon[32–35] have been prepared via ultrasonic spray pyrolysis (USP)[7] methods using molecular precursors to give uniquely structured materials (Figure S1). Here, we report a new, simple and versatile synthetic route to high surface area carbon microspheres that have hierarchical, mesoporous structure (**Figure 1**); and, we report their physicochemical and biological properties.

Titanium(IV) bis(ammonium lactato) dihydroxide[13] was diluted in water, aerosolized (nebulized) in air, and reacted using USP at two different temperatures (Figure 1). The synthetic result was the formation of TiO_2 nanoparticles that assemble into larger micrometer-sized spheres, a well-known outcome for aqueous aerosol synthesis methods.[1–9] The USP product color was gray to black indicating the presence of carbon. This was unexpected since the carrier gas was air and carbon syntheses predominantly occur under inert gas conditions.[36] A reasonable initial hypothesis was that at 850 °C, a

Dr. W. H. Suh, Prof. G. D. Stucky
Department of Chemistry & Biochemistry
Materials Department
University of California
Santa Barbara, CA 93106, USA
E-mail: stucky@chem.ucsb.edu; ws@berkeley.edu

Prof. J. K. Kang
NanoCentury KI and Graduate School of EEWS (WCU)
Department of Materials Science & Engineering
KAIST, Daejeon 305–701, Korea

Prof. Y.-H. Suh
Department of Pharmacology
College of Medicine
Seoul National University
28 Yeongeon-dong, Jongno-gu, Seoul, 110–799, Korea
E-mail: yhsuh@snu.ac.kr

Dr. W. H. Suh, Prof. M. Tirrell
Department of Bioengineering
University of California
Berkeley, CA 94720, USA

Prof. K. S. Suslick
School of Chemical Sciences
University of Illinois at Urbana-Champaign
600 S. Mathews Ave., Urbana, IL 61801, USA

core-shell structure resulted; a shell of TiO_2 solidified while carbon was being incorporated into a TiO_2 matrix towards the center of the microsphere. The TiO_2 shell, more than likely, acted as a barrier resulting in an oxygen free interior core condition and introduced a sub-micrometer level temperature gradient.

The formation of a TiO_2-carbon core structure (Figure 1,2) was confirmed via post-USP HF etching experiments. When chemically treated with 10% hydrogen fluoride (HF) for several hours, the core density of the 850 °C sample decreased. A sample made at 1000 °C, in contrast, displayed no apparent structural changes since the core TiO_2 was more crystalline, (and therefore etch resistant), and the carbon was burnt away (**Figure 2**, XRD data in Figures S2, S3). Concentrated HF treatment produced solid carbon spheres (Figure 1b, TEM, C-μS-850). If the reaction temperature was lowered to 400 °C, USP followed by etching produced a hollow carbon structure (Figure 1a, TEM, C-μS-400). Based on these results it was clear that a shell of crystalline TiO_2 was formed and a less crystalline TiO_2-carbon nanocomposite core was formed as the droplet of precursor solution underwent heating and consolidation. As mentioned earlier, we speculate that the solidified shell acted as a shield, inhibiting oxygen diffusion to the core and thereby reducing the core temperature. The carbon source comes from the TiO_2 precursor solution that incorporates monomeric lactate anions (chemical structure in Figure 1). These ligands, coordinated to Ti(IV), chemically polymerize and subsequently undergo anaerobic carbonization inside the TiO_2 shell. Lactate-like anions are known to form biodegradable copolymers at elevated temperatures or in the presence of a catalyst (e.g., Sn(IV)).[37]

Our report is a novel example of the formation of carbon microspheres using lactate as a carbon source under oxygenated conditions. There have been countless multistep efforts to create porous carbon[36,38–41] spheres based on resin co-polymerization processes and soft (i.e. surfactants such as F127 and P123)[42]/ hard template (i.e., SiO_2)[43] approaches under inert gas atmosphere. Our system utilizes a readily available molecular precursor and is highly reproducible, facile, and high yielding. Depending on the reaction temperature, the particle core is HF-soluble (i.e., at 400 °C, the degree of lactate polymerization at the core is low, affording only a shell to form at the interface), *multi-phased* (i.e., at 850 °C, nearly spherical carbon forms) or *phase-separated* (i.e., at 1000 °C, non-spherical carbon forms) (Figure 1, Figure 2), as is evident from the formation of spatially defined crystalline TiO_2 and carbon microspheres.
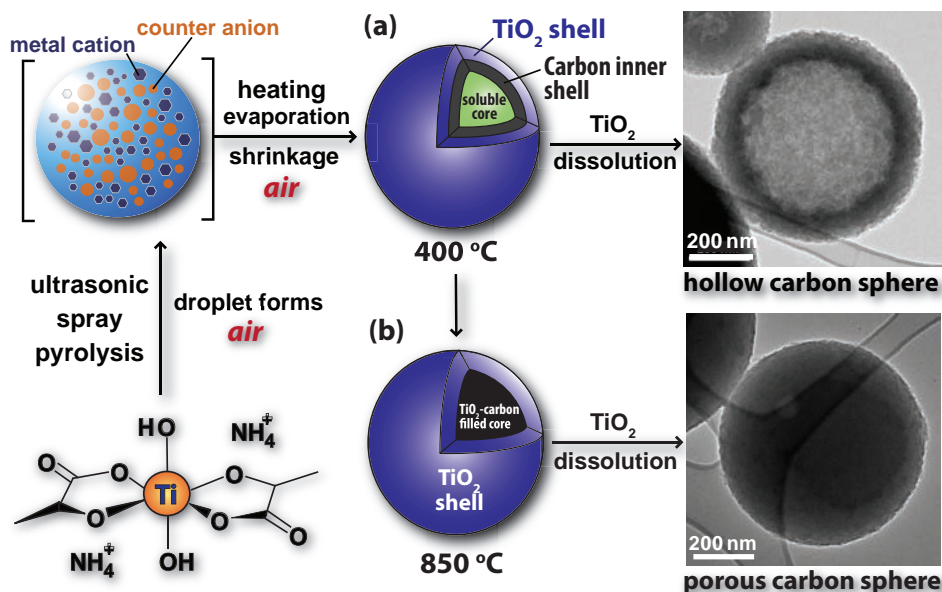
Figure 1. Hollow, Porous, and nanostructured Carbon Microspheres **(C-μS)**. Schematic routes for (a) hollow carbon (**C-μS-400**) and (b) porous carbon (**C-μS-850**). Respective transmission electron microscopy (TEM) images are on the far right.

Surface area analyses revealed that C-μS-850 yields mainly sub-3 nm pores (**Figure 3**) with a N_2 adsorption (BET) surface area of 1670 m^2/g, a pore volume of 1.06 cm^3/g, and an average pore diameter of 2.5 nm. The full isotherm curve is a cross between types I and IV, which means that the spheres have both micro- and mesoporosities (Figure 3). FT-IR analysis shows the presence of carboxylate and/or hydroxy functionality and C–H groups (Figure 3d) but after 50% HF treatment C-μS-850 does not incorporate any detectable Ti species (Figure 3e). We believe that the less crystalline TiO_2 nanoparticles present in the core act as an in situ sub-3 nm (hard) template (**Figure** 4a–f; enlarged in Figure S4, S5) with the formation of polylactide and

subsequent (incomplete) carbonization. This new one-pot core-shell phase separated approach can lead to other intriguing structures such as meso- and macroporous hollow TiO_2 spheres (Figure S6).

Microtome/TEM experiments (Figure 4) of a USP TiO_2-carbon 850 °C sample undisputedly show that the shell is comprised of strongly crystalline TiO_2 nanocrystals compared to the core (Figure 2, Figure 4a–f). Selected area electron diffraction (SAED) analyses show that highly crystalline TiO_2 phases are seen only in the shell and not the core (Figure 4a–f; enlarged in S4, S5). In contrast, the distinctive presence of void spaces was observed in the 1000 °C sample (Figure 4g–l; enlarged in
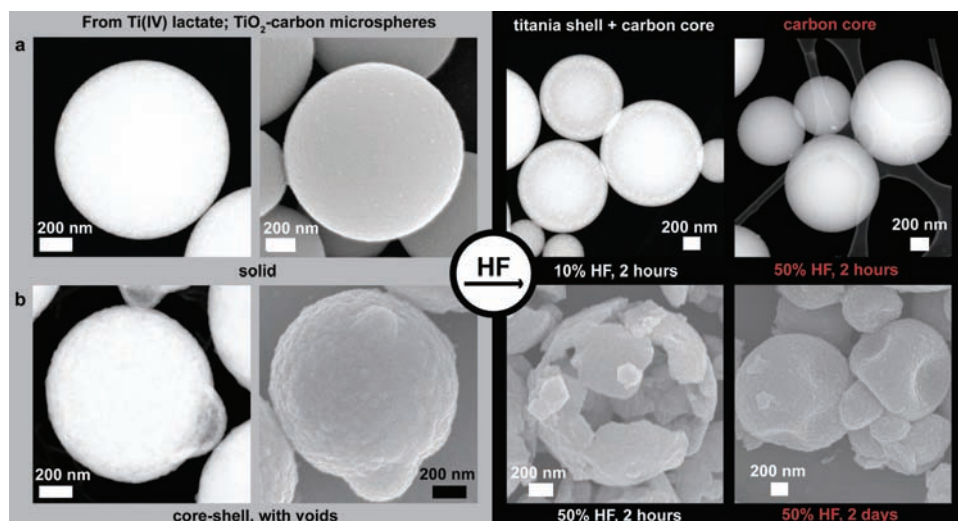

Figure 2. Etching experiments on microspheres prepared only with a Ti(IV) source. The TEM images show the microspheres before (left) and after etching (right) for TiO_2(-carbon) μS prepared at (a) 850 °C and (b) 1000 °C. Please refer to the main text and Supporting Information for additional details.

Materials
Views
www.MaterialsViews.com
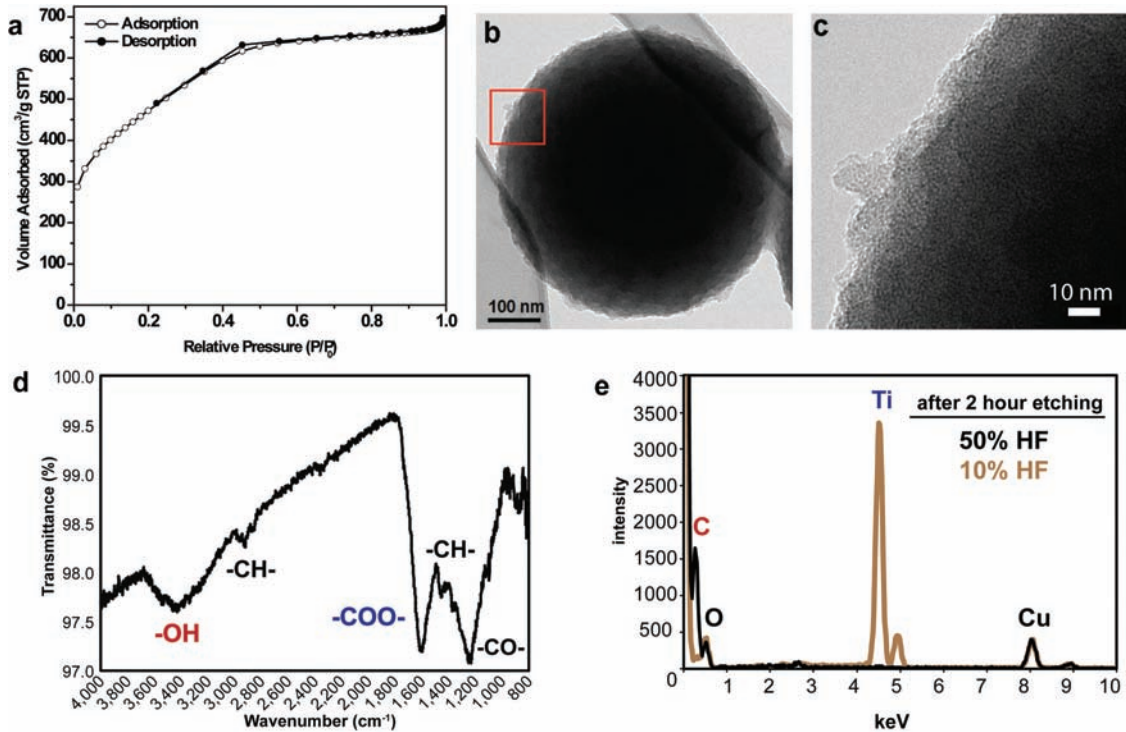
ADVANCED
MATERIALS
www.advmat.de

COMMUNICATION

Figure 3. Physicochemical properties of porous C-μS-850. (a) Nitrogen adsorption-desorption full isotherm curve is a cross between type I and IV. Data are consistent with reported systems.[36,40,42,43] (b) TEM of analyzed carbon sample. (c) TEM close-up showing 2–3 nm pores (red box in b). (d) FT-IR analysis result. (e) EDX analysis result. Details are in the main text.
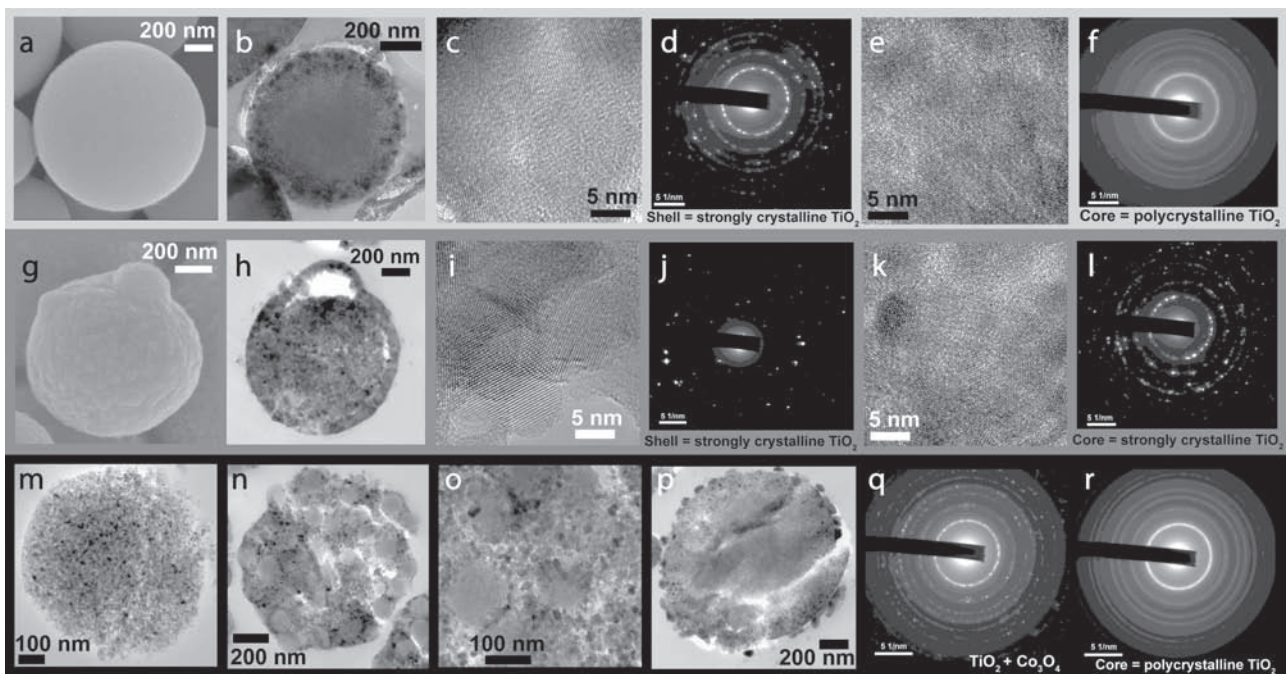

Figure 4. Microtoming, TEM, and SAED experimental results for USP TiO$_2$ μS. Ti(IV) lactate at 850°C: Whole particle (a) SEM, (b) TEM; high-resolution (c) TEM and (d) SAED of the shell; high-resolution (e) TEM and (f) SAED of the core. Ti(IV) lactate at 1000°C: Whole particle (g) SEM, (h) TEM; high-resolution (i) TEM and (j) SAED of the shell; high-resolution (k) TEM and (l) SAED of the core. 12 nm SiO$_2$ doped TiO$_2$ (μS-1): (m) TEM. 70–100 nm SiO$_2$ doped TiO$_2$ (μS-2): (n) whole particle TEM, (o) core close-up TEM. 12 nm SiO$_2$ and Co(II) doped TiO$_2$ (μS-3): (p) whole particle TEM, (q) shell SAED, and (r) core SAED.

S7, S8). In this case, the void space (Figure 2b, Figure 4h) was not filled with the epoxy resin, which was used to prepare the sample for microtoming. This is an indication that the shell formed at this temperature is practically non-porous. Since rutile phases are much more stable then anatase, additional etching process time was required for total TiO_2 dissolution (Figure 2, Figure 4; XRD in S2, S3).

Three different amorphous silica doped TiO_2 μS's (Figure S1) were additionally prepared[13] and their structures were analyzed (Figure 4m–r; enlarged in S9) via TEM in order to further understand the core-shell synthesis. For silica doped titania, μS-1 (12 nm) and μS-2 (70–100 nm), crystallinity was the same throughout the particle (Figure 4m–o; S1) whereas for 12 nm silica and Co(II) doped titania, μS-3, the result was similar to that obtained for the 850 °C USP TiO_2 sample. A more crystalline shell formed and then a polycrystalline core formed while Co_3O_4 formed on the exterior (Figure 4p–r; S1, S9).

Blending of the SiO_2 nanoparticles revealed that the aqueous-phase nanostructured TiO_2 USP synthesis affords the following three situations (Figure S1). Porous TiO_2 μS (Type II) can be synthesized using a precursor mixture of Ti(IV) and silica nanoparticles (5–100 nm). Since silica nanoparticles increase the thermal conductivity within the droplet, a temperature gradient does not readily form, though this depends on the doping level. The core and the shell experience similar temperatures, close to the surrounding gas temperature; we believe that the oxygen level should be the same as well. SiO_2 nanoparticles are encapsulated inside a crystalline TiO_2 microspherical matrix. Microtome experiments reveal that the crystallinities of the inner TiO_2 nanoparticles are similar to those in the shells (Figure 4m–o).

The core-shell microsphere synthesis can be summarized in the following manner (Figure S10). TiO_2-carbon core-shell μS (Type I) can be synthesized using a Ti(IV) precursor with an organic counter-anion (i.e. lactate). The shell formation occurs earlier, which creates a TiO_2-carbon nanocomposite. The core, which experiences a lower temperature than the shell, eventually solidifies but with less crystallinity. The resulting μS is composed of a strongly crystalline shell and a less polycrystalline core (Figure 4, and Supporting Information S4, S5). The formation of carbon within the core depends on the reaction temperature and concentration, since air will burn carbon at a faster rate in elevated temperatures and low concentrations.

For transition metal ion and nanoparticle doped TiO_2 synthesis (Type III), phase separation is induced possibly due to thermal conductivity and oxygen concentration perturbation. Especially in the Co(II) and 12 nm silica doped case,[13] sub-100 nm cobalt oxide nano-islands form on the exterior of the μS and subsequently act as an insulating/shielding layer to prevent heat and mass transport by plugging up pores in the shell. Thus, a shell of strongly crystalline TiO_2 forms first, then a less polycrystalline core forms later. Controlling the etching rates can either result in a hollow μS or a ball-in-ball μS with nanoparticles decorated on the outside (Figure 4p–r; S1b, S9).

In order to learn more about potentially useful properties of these novel materials, such as storage materials for small organic and biomolecules, the porous carbon microspheres were used in multiple adsorption experiments that include rhodamine 6G (R6G; fluorescent dye), thioflavin T (ThT; beta-sheet agglomerate binder), dehydroevodiamine hydrochloride

Table 1. Incorporation of Albumin-FITC and C16-W3K into porous C-μS-850 spheres.

Molecule	Particle	% Uptake
Albumin-FITC	SBA-15	15
	KIT-6	9
	FDU-12	1
	porous TiO_2 microsphere	0
	porous Carbon microsphere	98
C16-W3K	SBA-15	43
	KIT-6	26
	FDU-12	32
	porous TiO_2 microsphere	100
	porous carbon microsphere	67

(DHED; model Alzheimer's disease therapeutic candidate)[44], DHED sodium carboxylate (DHED-COONa, a DHED variant), albumin-FITC (a representative blood protein), and peptide amphiphile C16-Trp-Ala-Ala-Ala-Ala-Lys-Ala-Ala-Ala-Ala-Lys-Ala-Ala-Ala-Ala-Lys-Ala (C16-W3K; a bioactive lipid).[45,46] Unlike carbon nanotubes and other carbon materials, our carbon microspheres disperse well in aqueous media. FT-IR analysis of C-μS-850 revealed that carboxylate and/or hydroxy groups are present on the microspheres (Figure 3d) while EDX analysis showed the absence of Ti (Figure 3e); thus, C-μS-850 incorporates areas where polylactide was partially carbonized but without detectable TiO_2 nanoparticles. The percent uptake for representative small molecules R6G, ThT, DHED, and DHED-COONa were 100% at 5 μg/mL molecule concentration which well-exceeds the uptake limit of SBA-15,[47,48] KIT-6,[49,50] FDU-12,[51] and porous TiO_2 (USP) microspheres[13]–these latter examples typically uptake not more than 50%. **Table 1** summarizes comparison uptake experiments done using C16-W3K peptide amphiphile (represents lipids) and albumin-FITC (represents proteins). In addition, we tested the storage capacity for H_2, which was 0.047 wt% at room temperature and 0.15 wt% at 90 °C (at 28 Bar H_2 pressure). Bulk materials made from these carbon microspheres will not suffer from gas diffusion issues since gas molecules will not get captured inside the pores.[52,53] We conclude that our USP carbon microspheres have the capacity to store a broad variety of different molecules.

We envision using the high-surface-area carbon microspheres and hollow microspheres (average diameter ~1 μm) as binders to control the viscoelastic properties of biomimetic (hydro)gels for the construction of three-dimensional tissue scaffolds in vitro that can also achieve controlled release of bioactive molecules.[54–56] First, we confirmed through mammalian cell uptake experiments using murine microglia cell line BV-2 that our porous carbon microspheres, with or without incorporated molecules, are essentially non-cytotoxic (**Figure 5**a,b). Second, albumin-FITC incorporating C-μS-850 spheres were tested on human neural stem cell ReNcell VMs (here on ReNcells or hNSCs; Millipore, Inc.)[57] which showed that the carbon spheres are able to enter into hNSCs and deliver proteins without detrimental effects (Figure 5c, d).
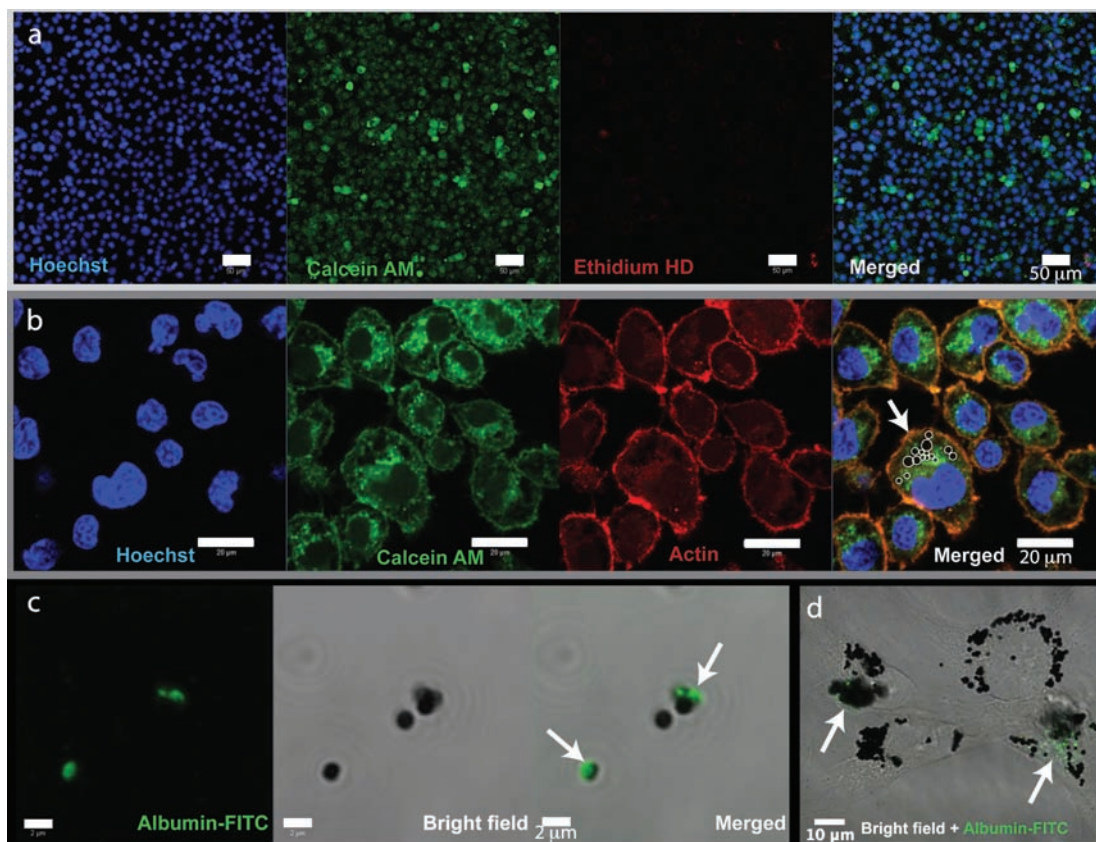
Figure 5. Carbon microsphere C-μS-850 treatment on murine microglia cells and human neural stem cells. BV-2 cells interfaced to C-μS-850 spheres analyzed by live/dead cell staining: (a) low and (b) high magnification images. (c) Five C-μS-850 spheres in liquid medium. Three spheres have Albumin-FITC adsorbed on the surface. (d) hNSCs with internalized CμS-850 spheres incorporating Albumin-FITC after two day incubation. Time lapse video of panels (c,d) (live cell imaging) and additional details are available as Supporting Information.

Exclusively on ReNcells, we conducted long-term interfacing and DNA transfection experiments (**Figure 6**). hNSCs grown on laminin were treated with C-μS-850 dispersed in sterile nanopure water. Growth factors (i.e. bFGF, EGF) were removed after one day of culture and the differentiation potential was compared. After more than a month of culture, the hNSCs were fixed and stained for specific markers (i.e., GFAP, Nestin, SNCA). Results showed that carbon-sphere-incorporating hNSCs did differentiate (Figure 6a,b) and stopped doubling; the control cells appeared to exhibit similar differentiation capacities while stopping cell division. Both the control (no treatment) and carbon treated cells expressed GFAP, Nestin (Figure 6c,d), and Sox-2 (weak, data not shown), levels identical under a confocal microscope. We also wanted to see the expression of alpha-synuclein (SNCA) proteins that are normally present in neural tissue. The aggregated or mis-folded forms of SNCA are implicated in Parkinson's disease and there is an increased interest of identifying the role of SNCA.[58–60] We confirmed the presence of SNCA in the nucleus of differentiated ReNcells and there was no real difference in the expression area and level (Figure 6c,d). We originally hypothesized that C-μS-850 may allow the amphiphilic SNCA protein to aggregate inside the cell and lead to cell death but the result showed that no SNCA, GFAP, or other proteins incorporated

into the carbon spheres. This prompted us to utilized C-μS-850 as hNSC transfection agents. Preliminary results suggest that (modified) C-μS-850 spheres are able to deliver (plasmid) DNA into ReNcells (Figure 6e,f) but at a sub-0.01% efficiency. The particular carbon spheres utilized for the successful transfection study were subject to fluorescein modification via surface carboxylate groups but no detectable fluorophore incorporation was observed. The chemically treated C-μS-850 spheres (e.g. peptide chemistry) were washed multiple times with nanopure water before hNSC experiments. Further hNSC transfection studies with carbon spheres are beyond the scope of this paper and we will report additional results in the near future.

In conclusion, studies of the USP TiO$_2$ μS structures[13] clearly show that the internal structure of a reacting droplet nebulized by a high-frequency ultrasound can be tuned. It is already known that cavitating bubbles produced by high intensity ultrasound (i.e., 20 kHz) are several micrometers in size, and have a temperature gradient.[61] Physical property confinement within a few micrometer sized spherical space is fascinating and we expect that further manipulations of this phenomena will be useful, particularly for USP since robust, porous and hollow TiO$_2$ nanostructured microspheres and high surface area carbon microspheres that are water-dispersible and
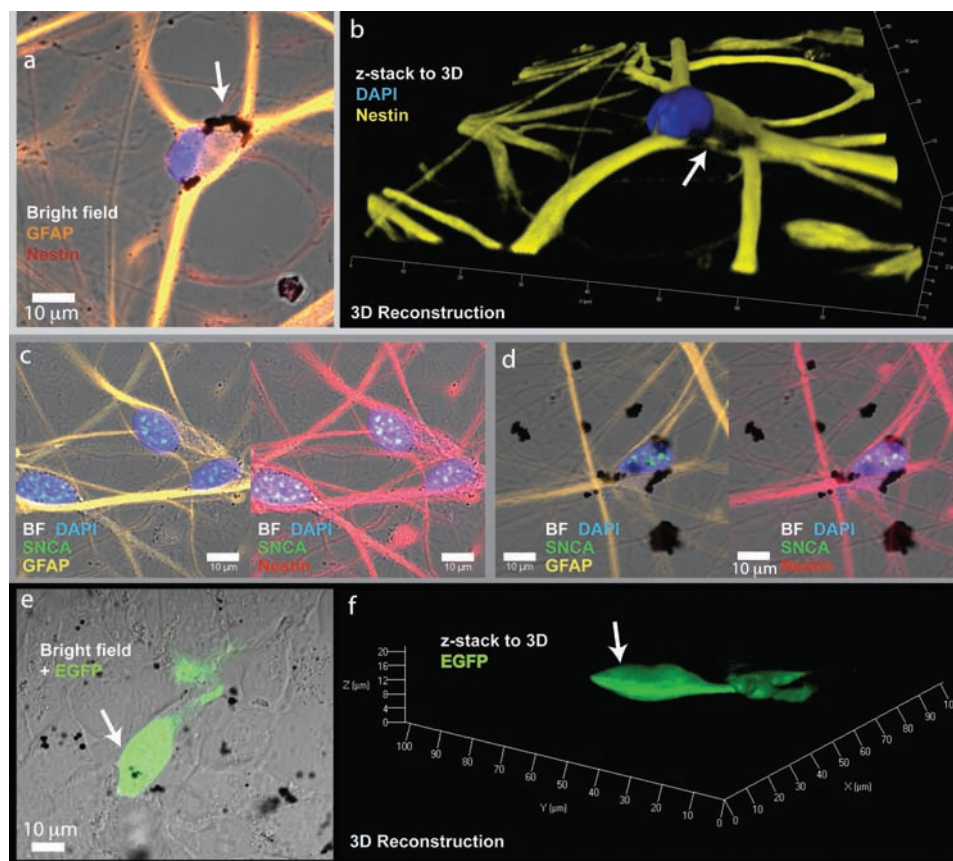
Figure 6. Long-term and transfection study on hNSCs after C-μS-850 treatment. ReNcell VM cells were subject to a month long culture after C-μS-850 carbon treatment and removal of growth factors. Row 1: (a) Differentiated NSC one month after carbon sphere interfacing. (b) 3D reconstruction; C-μS-850 spheres in arrow are inside the cell (arrow). Row 2: (c) Differentiated control hNSCs showing GFAP (yellow) and Nestin (red) expression. The green dots inside the nucleus represent SNCA. (d) Differentiated hNSC after C-μS-850 interfacing. Row 3: (e) A single hNSC expressing EGFP after one-day incubation with C-μS-850 and EGFP plasmids. (f) 3D reconstruction. Time-lapse video of EGFP expressing hNSC (e) and additional details are available as Supporting Information.

biocompatible can be synthesized using this approach in large quantities under oxygenic conditions.

Experimental Section

Details are available in the Supporting Information.

Supporting Information

Supporting Information is available from the Wiley Online Library or from the author.

Acknowledgements

[1] G. L. Messing, S. C. Zhang, G. V. Jayanthi, *J. Am. Ceram. Soc.* **1993**, *76*, 2707.

[2] T. T. Kodas, M. Hampden-Smith, *Aerosol Processing of Materials*, Wiley-VCH, NY **1999**.

[3] Y. Lu, H. Fan, A. Stump, T. L. Ward, T. Rieker, C. J. Brinker, *Nature* **1999**, *398*, 223.

[4] P. S. Patil, *Mater. Chem. Phys.* **1999**, *59*, 185.

[5] K. Okuyama, I. W. Lenggoro, *Chem. Eng. Sci.* **2003**, *58*, 537.

[6] W. H. Suh, Y. H. Suh, G. D. Stucky, *Nano Today* **2009**, *4*, 27.

[7] J. H. Bang, K. S. Suslick, *Adv. Mater.* **2010**, *22*, 1039.

[8] D. S. Jung, S. B. Park, Y. C. Kang, *Korean J. Chem. Eng.* **2010**, *27*, 1621.

[9] C. Boissiere, D. Grosso, A. Chaumonnot, L. Nicole, C. Sanchez, *Adv. Mater.* **2010**, *23*, 599.

[10] J. H. Lee, K. Y. Jung, S. B. Park, *J. Mater. Sci.* **1999**, *34*, 4089.

[11] Y. S. Chung, S. B. Park, D. W. Kang, *Mater. Chem. Phys.* **2004**, *86*, 375.

[12] V. Jokanovic, A. M. Spasic, D. Uskokovic, *J. Coll. Interfac. Sci.* **2004**, *278*, 342.

[13] W. H. Suh, A. R. Jang, Y. H. Suh, K. S. Suslick, *Adv. Mater.* **2006**, *18*, 1832.

[14] L. Li, C. K. Tsung, Z. Yang, G. D. Stucky, L. D. Sun, J. F. Wang, C. H. Yan, *Adv. Mater.* **2008**, *20*, 903.

[15] F. Iskandar, Mikrajuddin, K. Okuyama, *Nano Lett.* **2002**, *2*, 389.

[16] W. H. Suh, K. S. Suslick, *J. Am. Chem. Soc.* **2005**, *127*, 12007.

[17] L. Li, C. K. Tsung, T. Ming, Z. H. Sun, W. H. Ni, Q. Shi, G. D. Stucky, J. F. Wang, *Adv. Funct. Mater.* **2008**, *18*, 2956.

[18] V. Jokanovic, B. Jokanovic, *J. Optoelectron. Adv. Mater.* **2008**, *10*, 2684.

[19] S. Y. Lee, L. Gradon, S. Janeczko, F. Iskandar, K. Okuyama, *ACS Nano* **2010**, *4*, 4717.

[20] S. Gurmen, S. Stopic, B. Friedrich, *Mater. Res. Bull.* **2006**, *41*, 1882.

[21] S. W. Oh, H. J. Bang, Y. C. Bae, Y. K. Sun, *J. Power Sources* **2007**, *173*, 502.

[22] W. N. Wang, A. Purwanto, I. W. Lenggoro, K. Okuyama, H. Chang, H. D. Jang, *Ind. Eng. Chem. Res.* **2008**, *47*, 1650.

[23] J. M. Bian, X. M. Li, X. D. Gao, W. D. Yu, L. D. Chen, *Appl. Phys. Lett.* **2004**, *84*, 541.

[24] M. T. Htay, Y. Hashimoto, K. Ito, *Jpn. J. Appl. Phys. Part 1 – Regul. Pap. Brief Commun. Rev. Pap.* **2007**, *46*, 440.

[25] R. J. Helmich, K. S. Suslick, *Chem. Mater.* **2010**, *22*, 4835.

[26] A. Ortiz, J. C. Alonso, *J. Mater. Sci. Mater. Electron.* **2002**, *13*, 7.

[27] S. S. Dunkle, R. J. Helmich, K. S. Suslick, *J. Phys. Chem. C* **2009**, *113*, 11980.

[28] S. E. Skrabalak, K. S. Suslick, *J. Am. Chem. Soc.* **2005**, *127*, 9990.

[29] K. Okuyama, I. Wuled Lenggoro, N. Tagami, S. Tamaki, N. Tohge, *J. Mater. Sci.* **1997**, *32*, 1229.

[30] J. H. Bang, R. J. Helmich, K. S. Suslick, *Adv. Mater.* **2008**, *20*, 2599.

[31] P. P. Luz, A. M. Pires, O. A. Serra, *Quimica Nova* **2007**, *30*, 1744.

[32] S. E. Skrabalak, K. S. Suslick, *J. Am. Chem. Soc.* **2006**, *128*, 12642.

[33] R. B. Zheng, X. W. Meng, F. Q. Tang, L. Zhang, J. Ren, *J. Phys. Chem. C* **2009**, *113*, 13065.

[34] I. Khatri, T. Soga, T. Jimbo, S. Adhikari, H. R. Aryal, M. Umeno, *Diam. Relat. Mat.* **2009**, *18*, 319.

[35] M. E. Fortunato, M. Rostam-Abadi, K. S. Suslick, *Chem. Mater.* **2010**, *22*, 1610.

[36] J. Lee, J. Kim, T. Hyeon, *Adv. Mater.* **2006**, *18*, 2073.

[37] K. E. Uhrich, S. M. Cannizzaro, R. S. Langer, K. M. Shakesheff, *Chem. Rev.* **1999**, *99*, 3181.

[38] W. W. Lukens, G. D. Stucky, *Chem. Mater.* **2002**, *14*, 1665.

[39] C. Z. Yu, J. Fan, B. Z. Tian, D. Y. Zhao, G. D. Stucky, *Adv. Mater.* **2002**, *14*, 1742.

[40] Y. Deng, C. Liu, T. Yu, F. Liu, F. Zhang, Y. Wan, L. Zhang, C. Wang, B. Tu, P. A. Webley, H. Wang, D. Zhao, *Chem. Mater.* **2007**, *19*, 3271.

[41] Q. H. Shi, H. J. Liang, D. Feng, J. F. Wang, G. D. Stucky, *J. Am. Chem. Soc.* **2008**, *130*, 5034.

[42] Y. Yan, F. Zhang, Y. Meng, B. Tu, D. Zhao, *Chem. Commun.* **2007**, 2867.

[43] J. E. Hampsey, Q. Y. Hu, L. Rice, J. B. Pang, Z. W. Wu, Y. F. Lu, *Chem. Commun.* **2005**, 3606.

[44] C. H. Park, Y. J. Lee, S. H. Lee, S. H. Choi, H. S. Kim, S. J. Jeong, S. S. Kim, Y. H. Suh, *J. Neurochem.* **2000**, *74*, 244.

[45] T. Shimada, S. Lee, F. S. Bates, A. Hotta, M. Tirrell, *J. Phys. Chem. B* **2009**, *113*, 13711.

[46] M. Tirrell, in *AFIRM Annual Report*, (Ed: R. Vandre), **2009**, II-53 .

[47] D. Y. Zhao, Q. S. Huo, J. L. Feng, B. F. Chmelka, G. D. Stucky, *J. Am. Chem. Soc.* **1998**, *120*, 6024.

[48] D. Y. Zhao, J. L. Feng, Q. S. Huo, N. Melosh, G. H. Fredrickson, B. F. Chmelka, G. D. Stucky, *Science* **1998**, *279*, 548.

[49] R. Ryoo, S. Jun, J. M. Kim, M. J. Kim, *Chem. Commun.* **1997**, 2225.

[50] Y. F. Shi, B. K. Guo, S. A. Corr, Q. H. Shi, Y. S. Hu, K. R. Heier, L. Q. Chen, R. Seshadri, G. D. Stucky, *Nano Lett.* **2009**, *9*, 4215.

[51] T. Yu, H. Zhang, X. W. Yan, Z. X. Chen, X. D. Zou, P. Oleynikov, D. Y. Zhao, *J. Phys. Chem. B* **2006**, *110*, 21467.

[52] K. M. Thomas, *Dalton Trans.* **2009**, 1487.

[53] Y. Yurum, A. Taralp, T. N. Veziroglu, *Int. J. Hydrog. Energy* **2009**, *34*, 3784.

[54] Q. M. Jin, G. B. Wei, Z. Lin, J. V. Sugai, S. E. Lynch, P. X. Ma, W. V. Giannobile, *PLoS One* **2008**, *3*, e1729 .

[55] L. Ferreira, J. M. Karp, L. Nobre, R. Langer, *Cell Stem Cell* **2008**, *3*, 136.

[56] W. H. Suh, K. S. Suslick, G. D. Stucky, Y. H. Suh, *Prog. Neurobiol.* **2009**, *87*, 133.

[57] R. Donato, E. A. Miljan, S. J. Hines, S. Aouabdi, K. Pollock, S. Patel, F. A. Edwards, J. D. Sinden, *BMC Neurosci.* **2007**, *8*, 36 .

[58] M. G. Spillantini, M. L. Schmidt, V. M. Y. Lee, J. Q. Trojanowski, R. Jakes, M. Goedert, *Nature* **1997**, *388*, 839.

[59] Y. H. Suh, F. Checler, *Pharmacol. Rev.* **2002**, *54*, 469.

[60] F. Chiti, C. M. Dobson, *Annu. Rev. Biochem.* **2006**, *75*, 333.

[61] D. J. Flannigan, K. S. Suslick, *Nature* **2005**, *434*, 52.